2-2006

Chlorella virus MT325 encodes water and potassium channels that interact synergistically

Sabrina Gazzarrini
Università degli Studi di Milano

Ming Kang
University of Nebraska-Lincoln

Svetlana Epimashko
Università degli Studi di Milano

James L. Van Etten
University of Nebraska - Lincoln, jvanetten1@unl.edu

Jack Dainty
University of Toronto

See next page for additional authors

Chlorella virus MT325 encodes water and potassium channels that interact synergistically

Sabrina Gazzarrini[†], Ming Kang[‡], Svetlana Epimashko[†], James L. Van Etten[‡§], Jack Dainty[¶], Gerhard Thiel[‖], and Anna Moroni[†,††]

[†]Dipartimento di Biologia and Istituto di Biofisica–Consiglio Nazionale delle Ricerche, Università degli Studi di Milano, Via Celoria 26, 20133 Milan, Italy; [‡]Department of Plant Pathology and Nebraska Center of Virology, University of Nebraska, Lincoln, NE 68583-0722; [¶]Department of Botany, University of Toronto, 25 Willcocks Street, Toronto, ON, Canada M5S 3B2; [‖]Institute of Botany, Darmstadt University of Technology, 64287 Darmstadt, Germany; and [††]Istituto Nazionale per la Fisica della Materia, Unità di Milano-Università, Via Celoria 16, 20133 Milan, Italy

Contributed by James L. Van Etten, February 3, 2006

Fast and selective transport of water through cell membranes is facilitated by water channels. Water channels belonging to the major intrinsic proteins (MIPs) family have been found in all three domains of life, Archaea, Bacteria, and Eukarya. Here we show that *Chlorella* virus MT325 has a water channel gene, *aqpv1*, that forms a functional aquaglyceroporin in oocytes. *aqpv1* is transcribed during infection together with MT325 *kcv*, a gene encoding a previously undescribed type of viral potassium channel. Coexpression of AQPV1 and MT325-Kcv in *Xenopus* oocytes synergistically increases water transport, suggesting a possible concerted action of the two channels in the infection cycle. The two channels operate by a thermodynamically coupled mechanism that simultaneously alters water conductance and driving force for water movement. Considering the universal role of osmosis, this mechanism is relevant to any cell coexpressing water and potassium channels and could have pathological as well as basic physiological relevance.

water transport | aquaglyceroporins | membrane potential | osmoregulation | viroporin

Transport proteins facilitate fast passage of water, ions, and nutrients through membranes and are found in all living cells. Transport proteins are also encoded by some viruses, which are noncellular biological entities. Because viruses take over host cell functions to reproduce, transport proteins are probably used to modify the host cell environment to benefit virus replication. Viral transport proteins, known as viroporins, also exist in human pathogens such as HIV and influenza viruses (1). Viroporins are usually short peptides (<100 aa) with no structural analogies to prokaryotic and eukaryotic transport proteins. However, viroporins encoded by the *Phycodnaviridae* family (2) of nucleocytoplasmic large dsDNA viruses that infect algae are an exception. Genes encoding prokaryotic and eukaryotic-like membrane channels are present in some of the phycodnaviruses. We have previously shown that *Paramecium bursaria Chlorella* virus (PBCV-1), the prototype *Chlorella* virus (genus *Chlorovirus*), encodes a gene for a functional potassium ion (K^+) channel, Kcv (3, 4). Functional Kcv-like channels exist in 40 other *Chlorella* viruses infecting the same host (*Chlorella* NC64A) (5), as well as in another phycodnavirus, *Ectocarpus siliculosus* virus (6), which infects a marine filamentous brown alga. Here we report that phycodnavirus MT325, which infects *Chlorella* Pbi, has a functional water channel (ORF M30R) and a previously undescribed type of Kcv-like functional K^+ channel (ORF M183R), and that together these two channels improve water transport in *Xenopus* oocytes.

Results and Discussion

Virus MT325 ORF M30R encodes a 270-aa protein with homology to the major intrinsic proteins (MIPs) family. MIPs are present in all living organisms (7, 8), where they form water channels either selective for water (aquaporins) or glycerol-conducting channels, which also transport water, although to a lesser extent (aquaglyceroporins) (9). The viral MIP-like protein, named AQPV1 (aquaglyceroporin virus 1), was aligned and compared with the best-studied member of each group, aquaporin AQP1 (10, 11) from human and aquaglyceroporin GlpF (12) from *Escherichia coli* (Fig. 1*a*). AQPV1 has the main features of MIPs: six transmembrane domains (Fig. 1*b*) and the signature sequence Asn-Pro-Ala (NPA, highlighted in Fig. 1*a*) in both the amino- and carboxyl-terminal portions of the protein. These sequences are located in the channel pore of AQP1 and GlpF and play a crucial role in the orientation of water and glycerol molecules (13, 14). The narrowest part of the pore (the selectivity filter) is formed by four conserved amino acids with different physicochemical properties in aquaporins and aquaglyceroporins (12–15). AQPV1 has one polar (R^{217}) and three nonpolar (F^{49}, V^{202}, and I^{211}) residues (arrowheads in Fig. 1*a*) resembling the selectivity filter of aquaglyceroporins in these positions (15). Furthermore, AQPV1 contains five residues (in gray in Fig. 1*a*) that are conserved in aquaglyceroporins, but not in aquaporins (16, 17). Accordingly, a phylogenetic tree of aquaporins and aquaglyceroporins, places AQPV1 in the aquaglyceroporin cluster (Fig. 1*c*).

We performed hypotonic swelling assays in *Xenopus* oocytes injected with *aqpv1* cRNA to determine whether AQPV1 forms a functional water-conducting channel. The volume changes in oocytes were monitored in an osmotic gradient (ΔOsm = 105 milliosmolar) to quantify water permeability (P_f). Fig. 2*a* shows that the P_f value (in 10^{-4} cm·s^{-1}) of AQPV1-injected oocytes was 5 times higher than control oocytes (AQPV1 58 ± 3.5; control 11 ± 2). However, it was only ≈40% as high as AQP1-injected oocytes (151 ± 5), which were used as a reference for aquaporin-mediated water permeability (18). The water permeability of AQPV1 is high for aquaglyceroporins, which, with few exceptions (19), generally have ≈1/5 the water permeability of aquaporins (14, 20).

A point mutation N214A in the second AQPV1 NPA motif abolished the increase in P_f (6 ± 0.6). This result confirms the conclusion that the enhanced water permeability in AQPV1-injected oocytes is specifically induced by expression of this protein. Mercury, a classic inhibitor of water channels, reduced the P_f value of AQPV1-injected oocytes about 50% (*Inset* in Fig. 2*a*). This inhibition was partly reversed by the reducing com-

BIOPHYSICS

Conflict of interest statement: No conflicts declared.

Freely available online through the PNAS open access option.

Abbreviations: AQPV1, aquaglyceroporin *v*irus 1; Osm, osmolar; PBCV-1, *Paramecium bursaria Chlorella* virus.

Data deposition: The sequences reported in this paper have been deposited in the GenBank database (accession nos. DQ195162 for AQPV1 and DQ195163 for MT325-Kcv).

[§]To whom correspondence should be addressed at: Department of Plant Pathology, 406 Plant Sciences Hall, University of Nebraska, Lincoln, NE 68583-0722. E-mail: jvanetten@unlnotes.unl.edu.

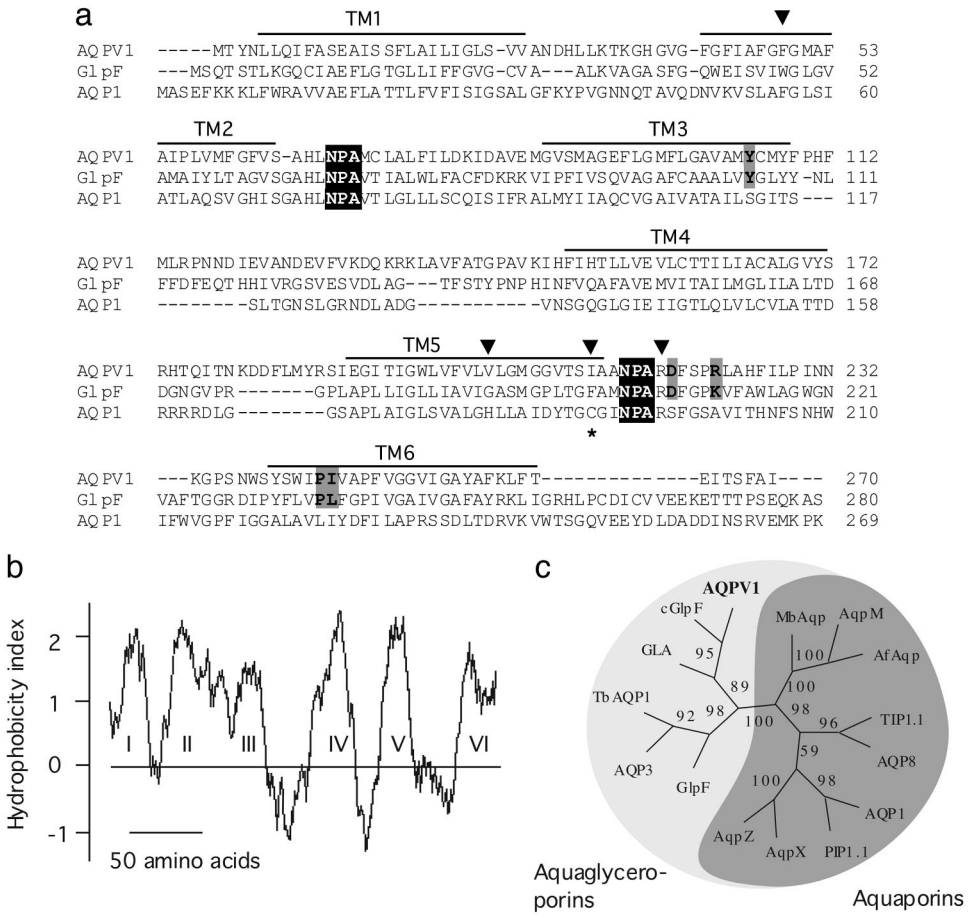

Fig. 1. Comparative alignment, predicted membrane topology, and phylogeny of AQPV1. (*a*) Multiple sequence alignment performed with CLUSTALW (1.82) of the deduced amino acid sequences of AQPV1 (GenBank accession no. DQ195162), the human aquaporin AQP1 (NP_932766) and the aquaglyceroporin GlpF from *E. coli* (NP_418362). Bold lines indicate the six transmembrane domains, TM1–TM6. The two NPA sequences, conserved in all water-channel proteins, are highlighted in black. Arrowheads identify four residues, F^{49}, V^{202}, I^{211}, and R^{217}, that are predicted to be part of the AQPV1 selectivity filter. Highlighted in gray are five amino acids highly conserved among aquaglyceroporins (16, 17). The asterisk indicates the cysteine residue responsible for AQP1 sensitivity to mercury (21). (*b*) Hydropathy profile of the deduced AQPV1 amino acid sequence predicted by the TMHMM program (www.cbs.dtu.dk/services/TMHMM/). The mean hydrophobicity index was computed according to the algorithm of Kyte and Doolittle (29) with a window of 17 residues. Putative membrane-spanning domains are numbered from I to VI and correspond to TM1–TM6 shown in *a*. (*c*) Neighbor-joining unrooted phylogenetic tree of 15 water channel protein sequences, including AQPV1. Multiple alignment was performed by using CLUSTALX with default settings. Phylogenetic analysis was performed by using PAUP 4.0b10. Numbers above the nodes are bootstrap values (1,000 replicates). Sequences are as follows: GlpF, *E. coli* (NP_418362); AQP3, *Homo sapiens* (CAI13311); TbAQP1, *Trypanosoma brucei* (AJ697889); GLA, *Lactococcus lactis* (P22094); cGlpF, *Clostridium acetobutylicum* (AAK79288); AQPV1, MT325 *Phycodnaviridae* (DQ195162); MbAqp, *Methanosarcina barkeri* (ZP_00077803); AqpM, *Methanothermobacter thermautotrophicus* (AB055880); AfAqp, *Archaeoglobus fulgidus* (NP_070255); TIP1.1, *Arabidopsis thaliana* (P25818); AQP8, *H. sapiens* (NP_001160); AQP1, *H. sapiens* (NP_932766); PIP1.1, *A. thaliana* (P61837); AqpX, *Brucella abortus* (Q9LA79); and AqpZ, *E. coli* (AAC43518). All proteins (except cGlpF) have been determined experimentally to be aquaporins or aquaglyceroporins.

pound 2-mercaptoethanol. The moderate inhibition of AQPV1 by this high (1 mM) concentration of mercury can be partly explained by the absence of a key cysteine residue (21) located near the carboxyl NPA motif of AQP1 (asterisk in Fig. 1*a*).

Glycerol uptake in AQPV1-injected oocytes was measured by incubating the cells in a solution containing 1 mM radiolabeled glycerol (1 μCi/ml [U-^{14}C]glycerol; 1 μCi = 37 kBq). AQPV1-injected oocytes accumulated glycerol rapidly (271 ± 8 pmol per oocyte per 15 min) (Fig. 2*b*). In contrast, glycerol uptake was low in control oocytes (53 ± 5 pmol per oocyte per 15 min), consistent with simple membrane diffusion. Similar low values were obtained for oocytes expressing AQP1 (66 ± 6 pmol per oocyte per 15 min), a water channel not permeable to glycerol and for the AQPV1 N214A mutant (23 ± 3 pmol per oocyte per 15 min). Hence the same mutation in the conserved pore domain of AQPV1 abolishes both water and glycerol transport. The glycerol uptake rate (V_i, pmol per oocyte per min) was linearly related to glycerol concentration in the solution (*Inset* in Fig. 2*b*). These results are qualitatively and quantitatively similar to those reported for other aquaglyceroporins (22).

Often water and K^+ channels are physically and functionally related to serve specific physiological functions in animal and plant cells (23, 24). The best-studied example is glial cells (23), where disturbances in the coupling between K^+ and water fluxes results in pathological formation of edema in retina and brain (25). Virus MT325 ORF M183R encodes a 95-aa protein, named MT325-Kcv, with ≈50% amino acid identity to the Kcv family of viral K^+ channels (3). Therefore, we determined if AQPV1 and MT325-Kcv might exhibit a functional relationship. However, it was first necessary to determine whether MT325-Kcv produced a functional K^+ channel in oocytes. The predicted structure of the 95-aa MT325-Kcv differs significantly from the 94-aa prototype viral K^+ channel PBCV-1-Kcv (Fig. 3*a*). MT325-Kcv lacks 10 aa at the amino terminus, predicted to form a slide helix required for PBCV-1-Kcv function (26); instead it contains 10 aa at the carboxyl terminus that are absent from PBCV-1-Kcv.

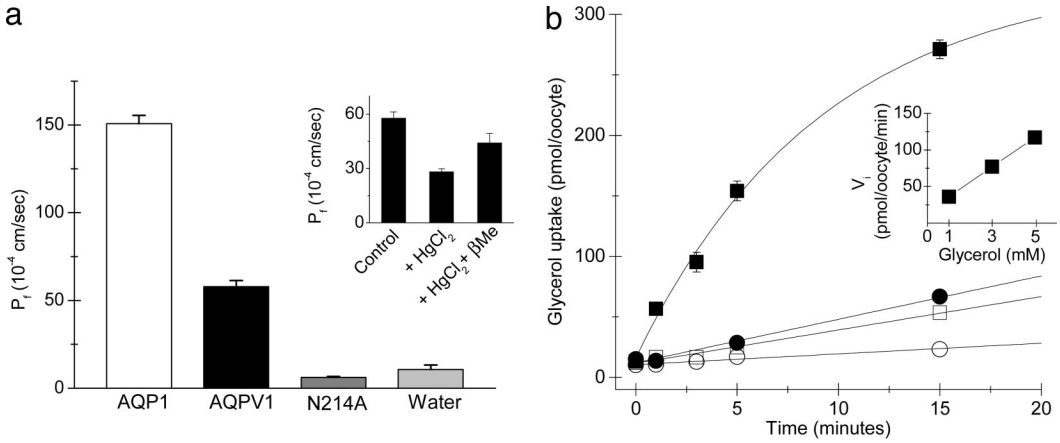

Fig. 2. Osmotic water permeability and glycerol uptake in AQPV1-injected oocytes. (*a*) Osmotic water permeability (P_f) of AQPV1-injected oocytes and comparison with human AQP1-injected oocytes. The mutation N214A in the highly conserved NPA motif reduces the P_f values of AQPV1-injected oocytes to below basal level (control: water-injected oocytes). Data are means ($n \geq 16$) for AQP1, AQPV1, N214A AQPV1, and water, respectively) ± SE of seven different experiments. (*Inset*) Pretreating AQPV1-injected oocytes with 1 mM $HgCl_2$ for 10 min reduced the P_f value by 50%. Partial recovery was observed after exposing the oocytes to 5 mM 2-mercaptoethanol (βMe) ($n \geq 10$). (*b*) Glycerol uptake kinetics in oocytes expressing AQPV1 (■), AQP1 (●), N214A AQPV1 (○), and control (water-injected) (□) oocytes. External glycerol concentration was 1 mM (1 μCi/ml [^{14}C]glycerol). Data are means ($n \geq 10$) ± SE of three independent experiments. When absent, SEs are within the symbols. (*Inset*) Effect of substrate concentration on glycerol uptake in AQPV1-injected oocytes. Initial velocity (V_i, pmol per oocyte per min) was determined from the initial slope of the time course of glycerol uptake experiments performed with 1, 3, and 5 mM glycerol. Values are means of five oocytes; SEs are within the symbols.

Despite these apparent structural differences, MT325-Kcv expression in oocytes produces a functional outwardly rectifying ion channel (Fig. 3 *b* and *c*). It is inhibited in a voltage-dependent manner by the classical K^+ channel blocker Ba^{2+}, resulting in 51 ± 8% ($n = 4$) inhibition at the free running membrane voltage (Fig. 3*c*). The channel is K^+-selective (ΔE_{rev} for 10-fold $\Delta[K^+]_{out}$ is 64 ± 1 mV, $n = 6$) and has a calculated permeability ratio, P_{Na}/P_K, of 0.01; furthermore, MT325-Kcv is not stretch-activated (Fig. 6, which is published as supporting information on the PNAS web site). We then examined the osmotic water permeability of oocytes coexpressing MT325-Kcv and AQPV1 (Fig. 3*d*). The P_f value in the coexpressing cells was 1.5 times

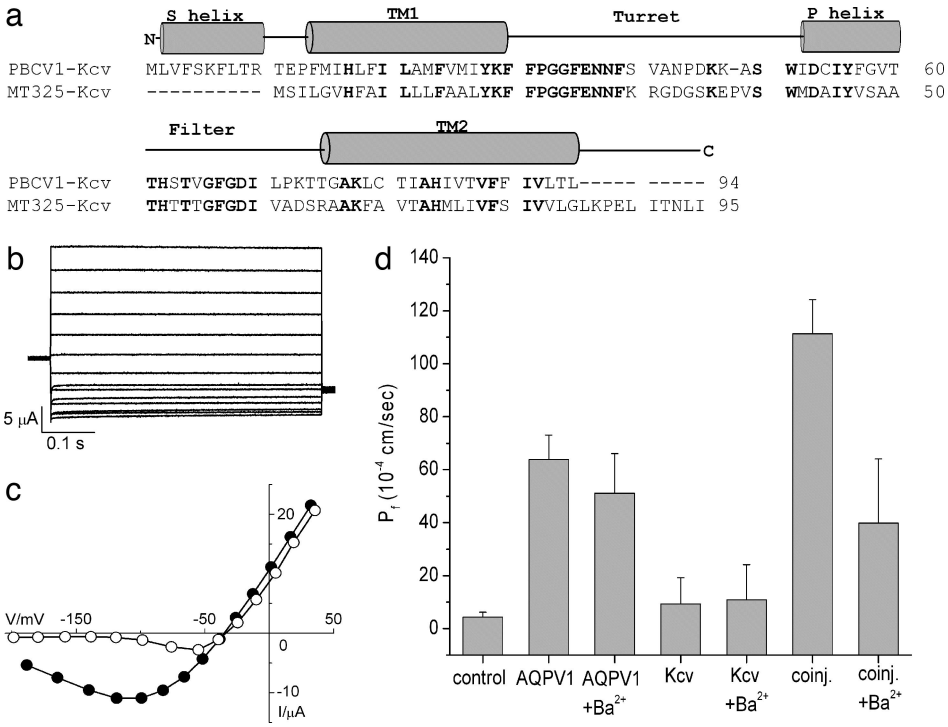

Fig. 3. Sequence alignment and properties of MT325-Kcv and its synergism with AQPV1. (*a*) Alignment of MT325-Kcv with PBCV1-Kcv, the functional K^+ channel protein from *Chlorella* virus PBCV-1 (3, 5). Identical amino acids are in boldface. The assignment of putative structural domains (Slide helix, TM1, Turret, Pore helix, Filter, and TM2) is based on a homology model of PBCV-1 Kcv with KirBac1.1 (30). The signature sequence of the selectivity filter of K^+ channels is TXXTXGY/FG (31). (*b*) Exemplary currents recorded by voltage clamp from a MT325-Kcv-injected oocyte in 20 mM external K^+. (*c*) Current (*I*)/voltage (*V*) relationship of the measurement shown in *b* (●) and the effect of 2 mM Ba^{2+} (○) in the external solution. (*d*) P_f measurements in control oocytes (water-injected) and oocytes injected with AQPV1 or MT325-Kcv (Kcv), or coinjected (coinj.) with AQPV1 and MT325-Kcv in the presence and absence of 2 mM Ba^{2+}. Data are means ($n \geq 3$) ± SE of three experiments.

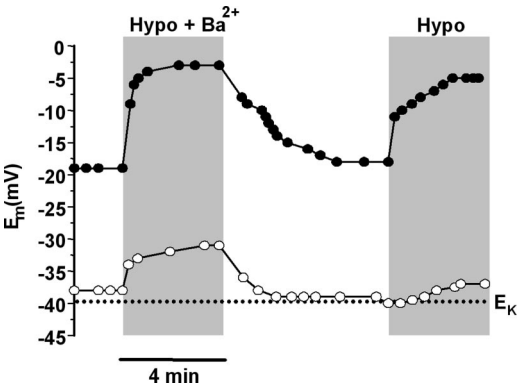

Fig. 4. Effect of hypoosmotic step on free running membrane potential (E_m) of oocytes injected with AQPV1 alone or coinjected with MT325-Kcv. Upper tracing (●) shows changes in time of the E_m values of a representative oocyte injected with AQPV1. At time 0 this oocyte rested in control solution (22 mM K^+, 215 mOsm) at −19 mV (−18.4 ± 1 mV, n = 21), a value far from the K^+ equilibrium voltage, E_K, shown by the dotted line [E_K = −40 mV, assuming $[K^+]_{in}$ is 100 mM (3)]. Exchange of control with hypoosmotic solution (Hypo, 22 mM K^+, 105 mOsm) indicated in the gray box, evoked a large depolarization (ΔE_m = 13 mV, mean ΔE_m = 9 ± 2 mV, n = 7). Depolarization was slightly higher (ΔE_m = 16 mV, mean = 12 ± 2 mV, n = 7) in the presence of 2 mM Ba^{2+} (Hypo + Ba^{2+}). The lower tracing (○) shows the E_m values of a representative oocyte coinjected with AQPV1 and MT325-Kcv. This cell rested in control solution at −38 mV (−38 ± 1 mV, n = 5), a value close to E_K. In hypoosmotic solution this value hardly moved from E_K (ΔE_m = 2.5 mV, mean = 4.2 ± 0.6, n = 6). The addition of 2 mM Ba^{2+}, which reduces MT325-Kcv conductance at E_m by about 50% (see text and Fig. 3*c*) allowed a significant depolarization, shifting E_m far positive of E_K (ΔE_m = 8 mV, mean = 12 ± 2.2 mV, n = 6); this condition, compatible with net K^+ efflux, abolished the synergistic effect of MT325-Kcv and AQPV1 on P_f (see text and Fig. 3*d*). Composition of solutions and experimental details are the same as for Fig. 3*d*. Free running membrane potential was measured with the voltage clamp amplifier in current clamp mode.

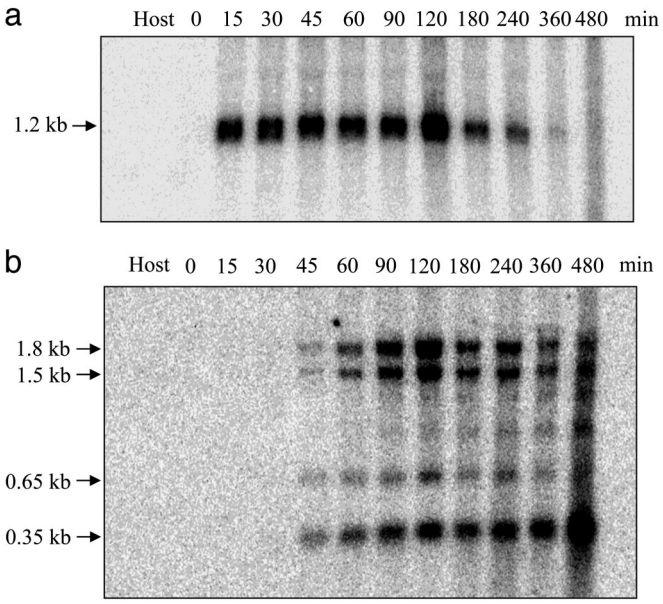

Fig. 5. Transcription pattern of *aqpv1* and MT325 *kcv* in the host *Chlorella* Pbi infected with virus MT325. (*a*) *Chlorella* Pbi (host) and Pbi virus MT325 RNAs hybridized with an *aqpv1* dsDNA probe. (*b*) *Chlorella* Pbi (host) and Pbi virus MT325 RNAs hybridized with MT325 *kcv* dsDNA probe. The *aqpv1* probe hybridized to a 1.2-kb band beginning at 15 min postinfection (p.i.) and increased in intensity to 120 min p.i., after which it decreased. Assuming the virus MT325 replication cycle is similar to that of virus PBCV-1, MT325 DNA synthesis begins 60–90 min p.i. Thus *aqpv1* is expressed as both an early and late gene. The ≈1.2-kb transcript is an appropriate size for a 270-aa protein. In comparison with transcription of *aqpv1*, that of the MT325 *kcv* gene is more complex. A *kcv* gene probe hybridized with four RNA bands, 1.8, 1.5, 0.65, and 0.35 kb, beginning about 45–60 min p.i. The three larger bands increased in intensity to 120 min p.i., after which they decreased. The 0.35-kb band, which is the size expected for a 95-aa protein, peaks in intensity at 480 min p.i. [Note: The PBCV-1 *kcv* gene also has a complex transcription pattern; however, a 0.35-kb RNA is expressed late and is the only one that is capped, indicative of a functional mRNA (32).]

higher than the sum of the P_f values from individual MT325-Kcv- and AQPV1-injected oocytes. Barium inhibited the synergistic effect produced by the two channels, indicating that MT325-Kcv stimulated water uptake (Fig. 3*d*).

How does an open K^+ channel increase water flow? In principle water flow can be elevated either by an increase in water conductance or by an increase in the osmotic driving force. MT325-Kcv does not transport water directly because the P_f value of oocytes expressing only the K^+ channel is similar to that of the control oocytes (Fig. 3*d*). In addition, MT325-Kcv does not indirectly increase the water conductivity of AQPV1: the P_f value of the coexpressing oocytes in the presence of Ba^{2+}, an inhibitor of MT325-Kcv, is not higher than that of oocytes expressing AQPV1 alone. Hence synergism must result from an increased osmotic driving force, greater than that of oocytes expressing AQPV1 alone. The apparent driving force is expressed by the factor α in Eq. **2** (see *Materials and Methods*). This factor accounts for changes in the osmotic driving force due to a fast endogenous osmoregulation of the oocytes. Osmoregulation is presumably relevant in oocytes undergoing dramatic and fast changes in volume due to the overexpression of water channels. Osmoregulation in oocytes implies the discharge of salts, mainly KCl, from the cell, decreasing the osmotic driving force for water and hence limiting the rate of swelling (27, 28). In AQPV1-expressing oocytes (without MT325-Kcv) the water flow is driven by $\alpha\Delta$Osm, where α is <1. With MT325-Kcv present the endogenous osmotic regulation is most likely suppressed because the membrane potential is clamped by the open channel to the K^+ equilibrium potential; in this situation there is no net movement of K^+ and for electroneutrality also no movement of its counterion Cl^-. The driving force is given by ΔOsm, i.e., α is 1 (Eq. **3**). Measurements of the free running membrane potential (E_m) of oocytes injected with MT325-Kcv and AQPV1 support this concept (Fig. 4). Oocytes expressing AQPV1 show E_m values positive of E_K and the potential value freely moves in hypoosmosis toward E_{Cl^-}, which in our conditions is close to zero. Net efflux of K^+ and Cl^- is allowed and endogenous osmoregulation can occur. In coinjected oocytes the presence of an open K^+ channel clamps the E_m value at E_K, preventing net flux of K^+ and its counterion Cl^-, both in control and in hypoosmotic solution. Partial reduction of the K^+ conductance by Ba^{2+} allows E_m to move positive of E_K, a condition that allows osmoregulation and abolishes synergism on water transport (Fig. 3*d*).

The synergistic function of the two channels raises the question whether they are expressed together during virus MT325 infection. To study this possibility, RNA was extracted from cells at various times after MT325 infection and hybridized to *aqpv1* and *kcv* gene probes. Both genes are expressed in MT325-infected cells and, although *aqpv1* is expressed earlier than *kcv*, expression of both transcripts overlaps at later stages of infection, consistent with a possible joint function (Fig. 5). Assuming that both channels are required for virus infection, AQPV1 and MT325-Kcv genes should be present in other viruses that infect *Chlorella* Pbi (Pbi viruses). To address this question we hybridized DNA from 47 additional Pbi viruses with the *aqpv1*- and *kcv*-specific probes. A positive signal was obtained with DNA from all of the Pbi viruses, but not the host (Fig. 7, which is published as supporting information on the PNAS web site). This finding supports the probable functional importance of both channels in the virus infection/replication processes.

Conclusions

Recent research has revealed the presence and functional importance of ion-conducting channels in several viruses, including a few that are medically important (1). The present work reveals that a virus encodes a functional water channel with a possible role in virus infection/replication. Our experiments also reveal a synergistic relationship between water and ion channels that provides the virus with a mechanism that controls transmembrane water fluxes by affecting water conductance and driving force. This mechanism could be relevant in any step in the life cycle of this and any other virus that involves osmotically driven processes. Furthermore, the coupling of K^+ conductance and water fluxes exemplifies a basic biological principle relevant to any physiological and pathophysiological situation involving cell volume changes and regulation.

Materials and Methods

Oocyte Expression. Capped cRNAs of AQP1, AQPV1, and MT325-Kcv were prepared as described in ref. 3. The point mutation in AQPV1 was created with the QuickChange site-directed mutagenesis kit (Stratagene). Oocytes were prepared from female *Xenopus laevis* as described (3) and injected with 50 nl of water or 10 ng of cRNAs (0.2 μg/μl). In coinjected oocytes, 10 ng of each cRNA was injected. Oocytes were incubated at 19°C in ND96 solution (96 mM NaCl/2 mM KCl/1.8 mM $CaCl_2$/1 mM $MgCl_2$/5 mM Hepes, adjusted to pH 7.5 with NaOH). The experiments were performed 3–4 days after injection.

Standard Oocyte Swelling Assays and P_f Calculations. The oocytes were placed in a chamber with 400 μl of ND96 solution (210 mOsm). At time 0, 200 μl of the solution was replaced by 200 μl of water to give a final osmolarity of 105 mOsm. The increase in oocyte volume was monitored at room temperature under an inverted microscope (Zeiss IM) with a ×2.5 magnifying objective lens and recorded by a charge-coupled device camera (Sony) connected to a computer through a WinTV-USB video-digitizer (Hauppauge, Hauppauge, NY). Two-minute movies of oocyte swelling were made with a sampling rate of one image per second. From sequential images, the surface areas of equatorial projections of the oocyte were estimated by using VIRTUALDUB (Avery Lee, Free Software Foundation, www.virtualdub.org) and IMAGEJ software (Wayne Rasband, National Institutes of Health, Bethesda). From these data, the oocyte volume was calculated, assuming that the oocyte was a sphere. The change in relative volume in the first 60 s $[d(V/V_0)/dt]$ was fitted to a linear regression giving the initial rates of swelling. According to Preston *et al.* (18), the osmotic water permeability P_f (10^{-4} cm·s^{-1}) was calculated from the initial rate of swelling $(d(V/V_0)/dt)$, initial volume (V_0), and initial surface area (S_0) of the oocyte (individually measured), the molar volume of water ($V_w = 18$ cm^3·mol^{-1}), and the osmotic gradient across the oocyte membrane (ΔOsm) by using the following formula:

$$P_f = [V_0 \times d(V/V_0)/dt]/(S_0 \times V_W \times \Delta\text{Osm}). \quad [1]$$

In the presence of fast endogenous osmoregulation, the osmotic gradient would be different from the applied and can be written as $\alpha\Delta$Osm; the swelling rate ($Y = V_0 \times d(V/V_0)/dt$), becomes

$$Y^* = P_f \times S_0 \times V_W \times \alpha\Delta\text{Osm}. \quad [2]$$

In ideal conditions, i.e., in the absence of oocyte endogenous osmoregulation, α is equal to 1 and the swelling rate is

$$Y = P_f \times S_0 \times V_W \times \Delta\text{Osm}. \quad [3]$$

Y^* equals the absolute swelling rate Y, when $\alpha = 1$, in the absence of osmoregulation.

When indicated, 1 mM $HgCl_2$ was added 10 min before the measurement and kept in the solution throughout the measurements. Five millimolar 2-mercaptoethanol was added to oocytes 15 min before the swelling assay, and oocytes were treated for 10 min with 1 mM $HgCl_2$ and washed with ND96 solution. The swelling assays reported in Fig. 3*d* were performed as follows: at time 0, 2/3 of isotonic solution (20 mM KCl/1.8 mM $CaCl_2$/1 mM $MgCl_2$/5 mM Hepes, pH 7.4 with KOH; osmolarity adjusted to 215 mOsm with mannitol) was replaced with hypotonic solution (20 mM KCl/1.8 mM $CaCl_2$/1 mM $MgCl_2$/5 mM Hepes, pH 7.4 with KOH, 55 mOsm) to give a final osmolarity of 105 mOsm. When present, $BaCl_2$ was added to a final concentration of 2 mM.

Glycerol Uptake of AQPV1 in Oocytes. For transport assays, five oocytes were washed and placed in 0.5 ml fresh ND96 solution. Glycerol uptake was started by replacing ND96 buffer with ND96 containing 1, 3, or 5 mM unlabeled glycerol and 1 μCi/ml [U-^{14}C]glycerol. Uptake of radiolabel glycerol was performed with moderate shaking at room temperature and stopped by washing the cells four times in a large excess (40 ml per washing) of ice-cold ND96 containing 100 mM unlabeled glycerol. Individual oocytes were dissolved overnight in 1 ml of 10% SDS and their radioactivities were measured.

Electrophysiology. Two-electrode voltage clamp was used to record K^+ currents from oocytes as described in refs. 3 and 5. Oocytes were perfused at room temperature with a solution containing 3, 20, 50, or 100 mM KCl, 1.8 mM $CaCl_2$, 1 mM $MgCl_2$, 5 mM Hepes, pH 7.4 with KOH, at a rate of 2 ml·min^{-1}. Mannitol was used to adjust the osmolarity to 215 mOsm. The clamp protocol consisted of 20-mV voltage steps from the holding voltage of −35 mV to voltages in the range +60 mV to −200 mV. Permeability ratios (P_{Na}/P_K) were calculated from data recorded in 50 mM KCl or NaCl solutions by using the following equation (31):

$$\Delta E_{rev} = E_{rev,Na} - E_{rev,K} = RT/zF \ln P_{Na}[\text{Na}]_0/P_K[K]_0\,, \quad [4]$$

where E_{rev} is the value in millivolts of the current reversal potential measured in the presence of 50 mM monovalent cation (either Na^+ or K^+); $[Na]_o$ and $[K]_o$ are the cations' concentrations in the external solution; and R, T, z, and F have their usual thermodynamic meanings.

We thank Mike Nelson for collecting many of the viruses that infect *Chlorella* Pbi, including virus MT325; Roberto Marotta for helping with the phylogenetic tree; Ralf Kaldenhoff for providing AQP1; and Daniele Gaslini for technical help. This investigation was supported in part by National Institutes of Health Grant GM32441 (to J.L.V.E.), by the Center of Biomedical Research Excellence program of the National Center for Research Resources Grant P20-RR15635 (to J.L.V.E.), and by Ministero dell'Istruzione, dell'Universita e della Ricerca Grant RBAU01JT9C (to A.M.).

1. Gonzalez, M. E. & Carrasco, L. (2003) *FEBS Lett.* **552,** 28–34.
2. Van Etten, J. L. & Meints, R. H. (1999) *Annu. Rev. Microbiol.* **53,** 447–494.
3. Plugge B., Gazzarrini, S., Nelson, M., Cerana, R., Van Etten, J. L., Derst, C., DiFrancesco, D., Moroni, A. & Thiel, G. (2000) *Science* **287,** 1641–1644.
4. Kang, M., Moroni, A., Gazzarrini, S. & Van Etten, J. L. (2003) *FEBS Lett.* **552,** 2–6.
5. Kang, M., Moroni, A., Gazzarrini, S., DiFrancesco, D., Thiel, G., Severino, M. & Van Etten, J. L. (2004) *Proc. Natl. Acad. Sci. USA* **101,** 5318–5324.
6. Chen, J., Cassar, S. C., Zhang, D. & Gopalakrishnan, M. (2005) *Biochem. Biophys. Res. Commun.* **326,** 887–893.
7. Borgnia, M., Nielsen, S., Engel, A. & Agre, P. (1999) *Annu. Rev. Biochem.* **68,** 425–458.
8. Kozono, D., Ding, X., Iwasaki, I., Meng, X., Kamagata, Y., Agre, P. & Kitagawa, Y. (2003) *J. Biol. Chem.* **278,** 10649–10656.
9. Agre, P., Bonhivers, M. & Borgnia, M.J. (1998) *J. Biol. Chem.* **273,** 14659–14662.

10. Cheng, A., van Hoek, A. N., Yeager, M., Verkman, A. S. & Mitra, A. K. (1997) *Nature* **387,** 627–630.
11. Murata, K., Mitsuoka, K., Hirai, T., Walz, T., Agre, P., Heymann, J. B., Engel, A. & Fujiyoshi, Y. (2000) *Nature* **407,** 599–605.
12. Fu, D., Libson, A., Miercke, L. J., Weitzman, C., Nollert, P., Krucinski, J. & Stroud, R. M. (2000) *Science* **290,** 481–486.
13. Sui, H., Han, B.-G., Lee, J. K., Wallan, P. & Jap, B. K. (2001) *Nature* **414,** 872–878.
14. Nollert, P., Harries, W. E. C., Fu, D., Miercke, L. J. W. & Stroud, R. M. (2002) *FEBS Lett.* **504,** 112–117.
15. Thomas, D., Bron, P., Ranchy, G., Duchesne, L., Cavalier, A., Rolland, J. P., Raguenes-Nicol, C., Hubert, J, F., Haase, W. & Delamarche, C. (2002) *Biochim. Biophys. Acta* **1555,** 181–186.
16. Froger, A., Tallur, B., Thomas, D. & Delamarche, C. (1998) *Protein. Sci.* **7,** 1458–1468.
17. Lagreé, V., Froger, A., Deschamps, S., Hubert, J. F., Delamarche, C., Bonnec, G., Thomas, D., Gouranton, J. & Pellerin, I. (1999) *J. Biol. Chem.* **274,** 6817–6819.
18. Preston, G. M., Carroll, T. P., Guggino, W. B. & Agre, P. (1992) *Science* **256,** 385–387.
19. Hansen, M., Kun, J. F., Schultz, J. E. & Beitz, E. (2002) *J. Biol. Chem.* **277,** 4874–4882.
20. Maurel, C., Reizer, J., Schroeder, J. I., Chrispeels, M. J. & Saier, M. H., Jr. (1994) *J. Biol. Chem.* **269,** 11869–11872.
21. Preston, G. M., Jung, J. S., Guggino, W. B. & Agre, P. (1993) *J. Biol. Chem.* **268,** 17–20.
22. Uzcategui, N. L., Szallies, A., Pavlovic-Djuranovic, S., Palmada, M., Figarella, K., Boehmer, C., Lang, F., Beitz, E. & Duszenko, M. (2004) *J. Biol. Chem.* **279,** 42669–42676.
23. Nagelhus, E. A., Mathiisen, T. M. & Ottersen, O. P. (2004) *Neuroscience* **129,** 905–913.
24. Maurel, C. (1997) *Annu. Rev. Plant Physiol. Plant Mol. Biol.* **48,** 399–429.
25. Pannicke, T., Iandiev, I., Uckermann, O., Biedermann, B., Kutzera, F., Wiedermann, P., Wolburg, H., Reichenbach, A. & Bringmann, A. (2004) *Mol. Cell. Neurosci.* **26,** 493–502.
26. Moroni, A., Viscomi, C., Sangiorgio, V., Pagliuca, C., Meckel, T., Horvath, F., Gazzarrini, S., Valbuzzi, P., Van Etten, J. L., DiFrancesco, D. & Thiel, G. (2002) *FEBS Lett.* **530,** 65–69.
27. Ackerman, M. J., Krapivinsky, G. B., Gordon, E., Krapivinsky, L. & Clapham, D. C. (1994) *Jpn. J. Physiol* **44,** S17–S24.
28. Ackerman, M. J., Wickman, K. D. & Clapham, D. E. (1994) *J. Gen. Physiol.* **103,** 153–179.
29. Kyte, J. & Doolittle, R. F. (1982) *J. Mol. Biol.* **157,** 105–132.
30. Gazzarrini, S., Kang, M., Van Etten, J. L., DiFrancesco, D., Tayefeh, S., Kast, S. M., Thiel, G. & Moroni, A. (2004) *J. Biol. Chem.* **279,** 28443–28449.
31. Hille, B. (2001) *Ion Channels of Excitable Membranes* (Sinauer, Sunderland, MA).
32. Kang, M., Graves, M., Mehmel, M., Moroni, A., Gazzarrini, S., Thiel, G., Gurnon, J. G. & Van Etten, J. L. (2004) *Virology* **326,** 150–159.

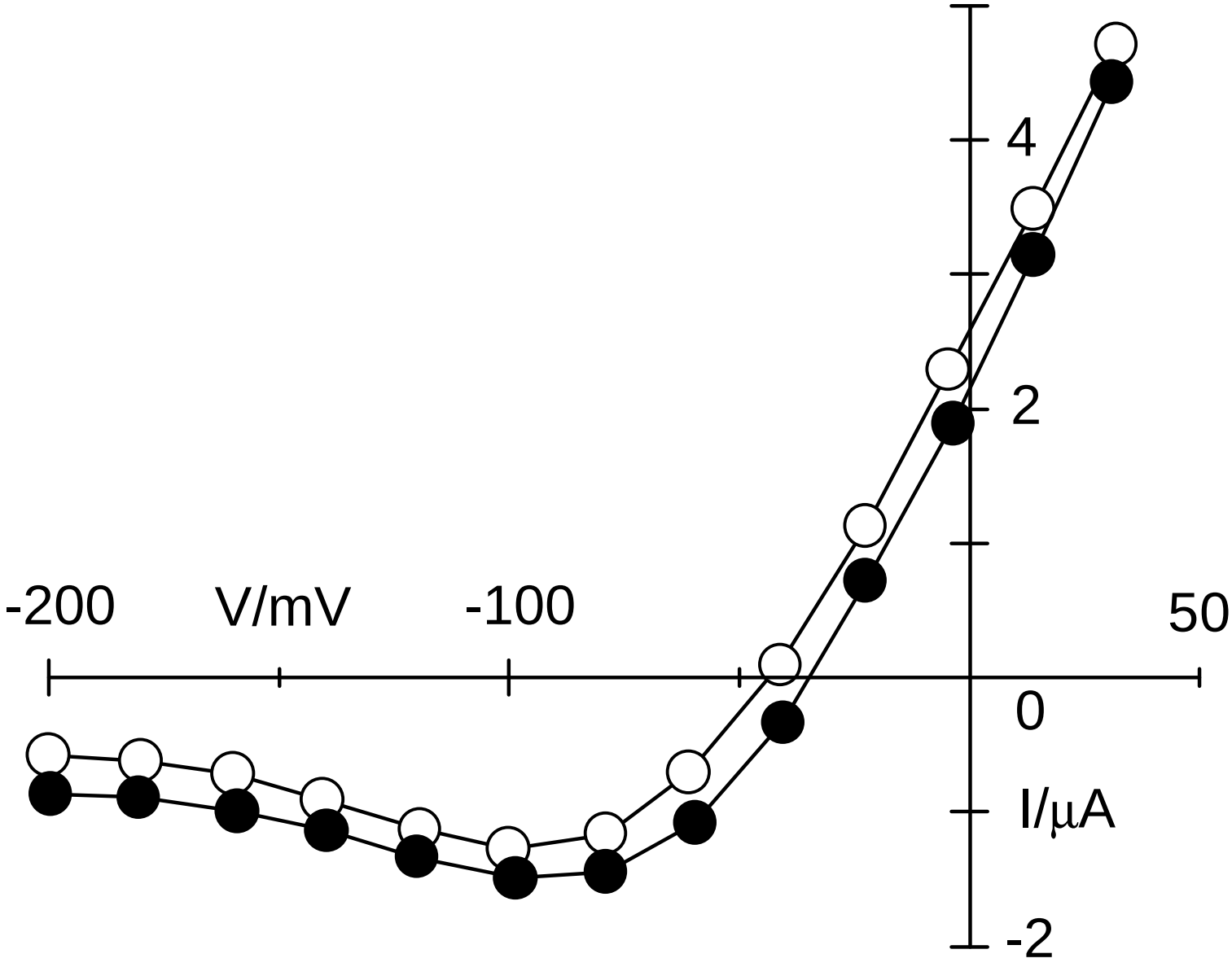
4
2
-200
V/mV
-100
50
0
I/μA
-2

Dot Blot Hybridizations of Pbi Viral DNAs against MT325 AQPV1 Gene Probe

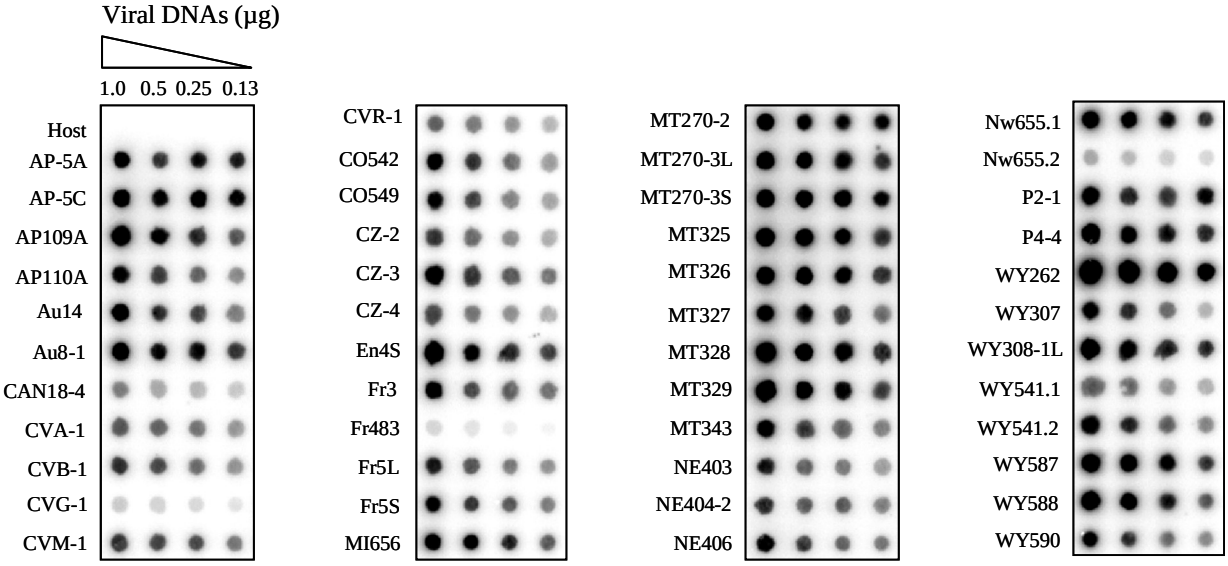

Dot Blot Hybridizations of Pbi Viral DNAs against MT325-Kcv Gene Probe